NPL REPORT CETM 18

Effect on the E-field distribution of ferrite tiling on the walls of the MEB 1750 GTEM cell

SH Fletcher, MJ Alexander, JC Jee,
W Liang, BG Loader

March 2000

Effect on the E-field distribution of ferrite tiling on the walls of the MEB 1750 GTEM cell

By

S H Fletcher, B G Loader, W Liang, M J Alexander, J C Jee

CENTRE FOR ELECTROMAGNETIC METROLOGY
NATIONAL PHYSICAL LABORATORY
Teddington, TW11 0LW

ABSTRACT

GTEM cells (GigaHertz Transverse ElectroMagnetic) devices are used by EMC test houses to carry out EMC radiated immunity testing and also for measuring radiated emissions from electrical products. They provide a compact alternative to measuring on Open Area Test Sites (OATS) or anechoic chambers and are free from the effects of ambient interference as found on OATS. GTEMs are suggested as alternative test sites in IEC standards however, despite being in existence for over ten years, there are still some problems to be resolved. The most notable is a significant longitudinal **E**-field component that appears at different frequencies depending on the size of the GTEM. The cell used at NPL is the MEB GTEM 1750, which displays this cross-polar component at around 125 MHz. A possible solution is presented in this report, that of lining the side walls of the GTEM with ferrite absorber tiles in the expectation that this will reduce the cross-polar component without significantly reducing the vertical **E**-field.

ISSN 1467-3932

National Physical Laboratory
Teddington, Middlesex, UK, TW11 0LW

Switchboard 020 8977 3222

.

Approved on behalf of the Managing Director, NPL, by Dr S Pollitt
Head of the Centre for Electromagnetic and Time Metrology.

Table of Contents

1. Introduction

A longitudinal **E**-field component has been observed in a variety of GTEM cells of various sizes produced by various manufacturers and measured by various test laboratories. As a result it is accepted that the cause is inherent to the cells, rather than related to the measurement technique. The frequency at which it appears is related to the dimensions of the cell. In the GTEM 1750 described in this report, this component appears at 125 MHz at the centre of the measurement plane (See Section 2.1). This frequency is within the range used for testing many EUTs, so it would be valuable to either eliminate this effect, or derive a correction term that could be applied to all measurements.

Results are given of extensive field-mapping in the GTEM to accurately characterise the field around the measurement point using a semi-automated scanner. This was carried out in the unlined GTEM and then repeated after ferrite absorber tiles had been attached to the GTEM walls in an attempt to reduce the longitudinal component. The scanner was developed at NPL and controlled by a Visual Basic program also written by NPL. An isotropic **E**-field probe, the FP-2000, was positioned on a wooden support which can be moved transversely across the cell, and the probe itself can be moved up and down the support pole. At present, the transverse position can be controlled by the program, as can the frequency range and step size, but the height must be adjusted manually.

For the purposes of this investigation, measurements were taken at a large number of positions in and around the measurement plane (See Section 2.1). The power input to the cell was recorded. The three orthogonal components of the **E**-field are also recorded, as well as the isotropic value. Separate TDR measurements were also made in the empty and tiled cell, and these were used to derive the impedance of the two states of the cell. The measurements described have produced a large amount of data which has been processed for a specific purpose. It may prove useful to examine other properties of the cell using the data acquired here. This is discussed in the conclusions.

2. Measurement system

2.1 Measurement plane of the GTEM

The measurement plane of the cell is the plane where most measurements were carried out. There is not a complete consensus among UK GTEM users on the definition of the co-ordinates of the measurement plane. The *y* (vertical) origin is always halfway between the GTEM floor and septum, and the *x* (transverse) origin is on the longitudinal axis. For the purposes of this investigation the central *z* co-ordinate is defined as being the position where a line projected in the *x*-direction from the centre of the cell door crosses the longitudinal axis. This is shown in Figure 1 where the dot represents the centre point. The measurement plane is extended by a distance of ± *d*/6 in both *x* and *y* directions, where *d* is the floor to septum separation.

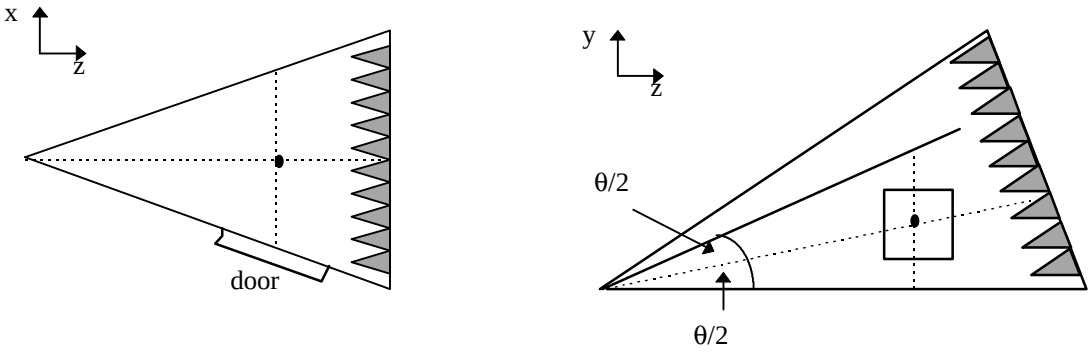

Figure 1 : Definition of GTEM centre point, plan view and cut away.

2.2 The physical measurement system

The measurement system used is shown in Figures 2 and 3. One curtain rail was attached to the floor of the cell and one to the septum. A third curtain rail was attached to a piece of balsa wood, one end of which was attached to the rail on the septum and the other end to the rail on the floor. Note that the co-ordinates of the FP-2000 are not the same as those defined for the GTEM. This was not possible for technical reasons. The Cartesian co-ordinates in the cell are defined as *x* is transverse, *y* is vertical and *z* is longitudinal (see Figure 1, above). If the co-ordinates of the FP-2000 are annotated *x*′, *y*′ and *z*′, then

x′ = *y*
y′ = *x*
z′ = *z*

Unless stated otherwise, all co-ordinates refer to the GTEM system.

To obey the boundary conditions of Maxwells equations the **E**-field must be perpendicular to the septum and the GTEM floor, which will produce a spherical

wavefront in an unmoded GTEM. The scan plane is set up such that the central position is orthogonal to the direction of propagation of the **E**-field in the cell, which in this case is 6.7°.

For the purposes of this report the frequency range was set from 100 MHz to 1 GHz, measuring in 100 MHz steps. The probe was measured in 21 positions 10 cm apart in the transverse direction, from -1 m to + 1 m. This was repeated at 11 heights, again in 10 cm steps, from - 0.5 m to + 0.5 m with respect to the centre. This gave a total of 231 positions in the measurement plane, at 10 frequencies. This was carried out in the empty cell, after one cell wall had been tiled, and when the cell was fully tiled.

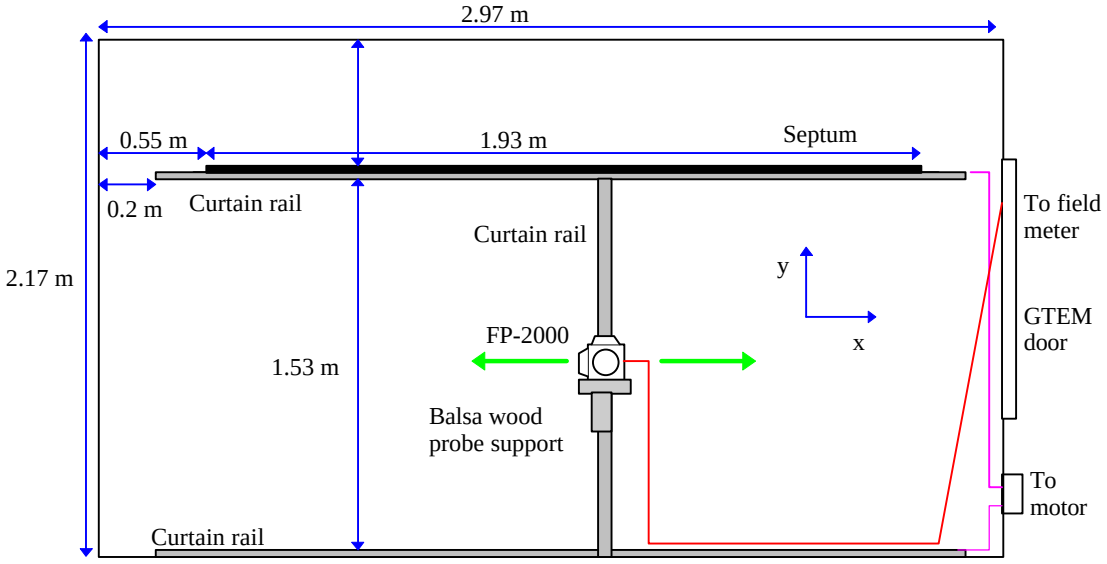

Figure 2 : Diagram of the scanner system utilised in the NPL GTEM, looking from the tip towards the RAM.

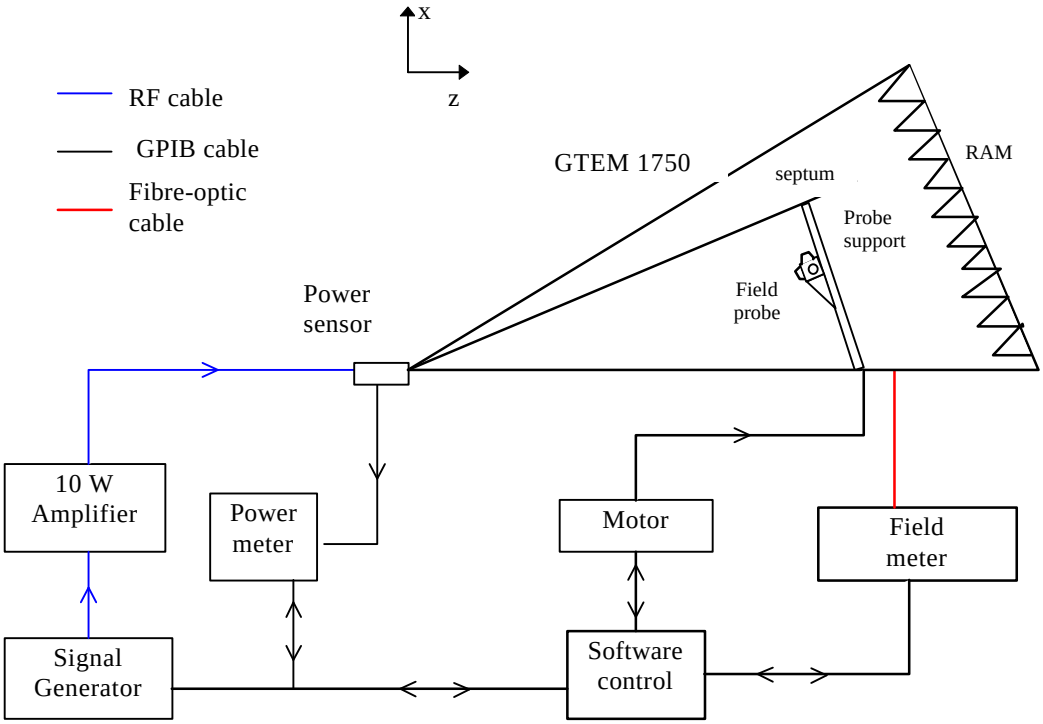

Figure 3 : Cutaway of GTEM cell and external control system.

The scanner is controlled by a visual basic program. The program is designed to produce the same input power to the cell for a given frequency such that the **E**-field strength at the centre of the cell remains constant throughout the scan. This is achieved by monitoring the power sensor reading, proportional to the input power into the cell, and adjusting the output power of the signal generator.

The positioning and distance stepping of the probe in the cell as well as the frequencies and the frequency stepping are user defined. The parts of the scanner inside the cell are made from plastic and wood so the field will not be perturbed. A string and pulley within the curtain rails allows for transverse movement using the motor which is attached to the outside of the GTEM. It would be possible to also control the vertical position of the probe, but this was found to be too time-consuming to implement and therefore the height was set manually.

2.3 Adding ferrite tiles to the cell

Measurements were taken initially in the untiled cell, then with one wall tiled, and finally in the fully tiled cell. The wall not containing the door was tiled first, and the tiling configuration is shown in Figure 4 below.

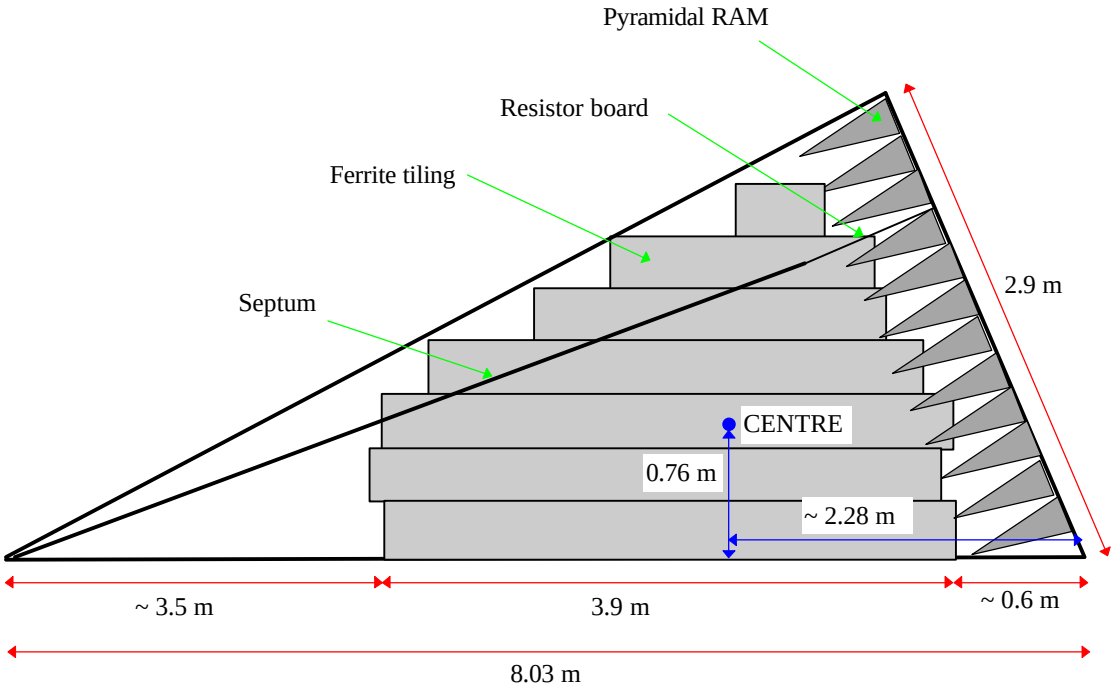

Figure 4 : Configuration of ferrite absorber tiles on side wall opposite the door

The Toyo absorber tiles each measure $10 \times 10 \times 2$ cm and are in 3×3 blocks. A sheet of plywood was attached to the cell wall and the tiles screwed onto this. This wall has a total of 585 individual tiles in 65 3×3 blocks. The tiles add considerable weight to the GTEM so additional wooden supports were added underneath the GTEM to prevent damage to the existing legs. The configuration of tiles on the wall containing the door is shown in Figure 5 below.

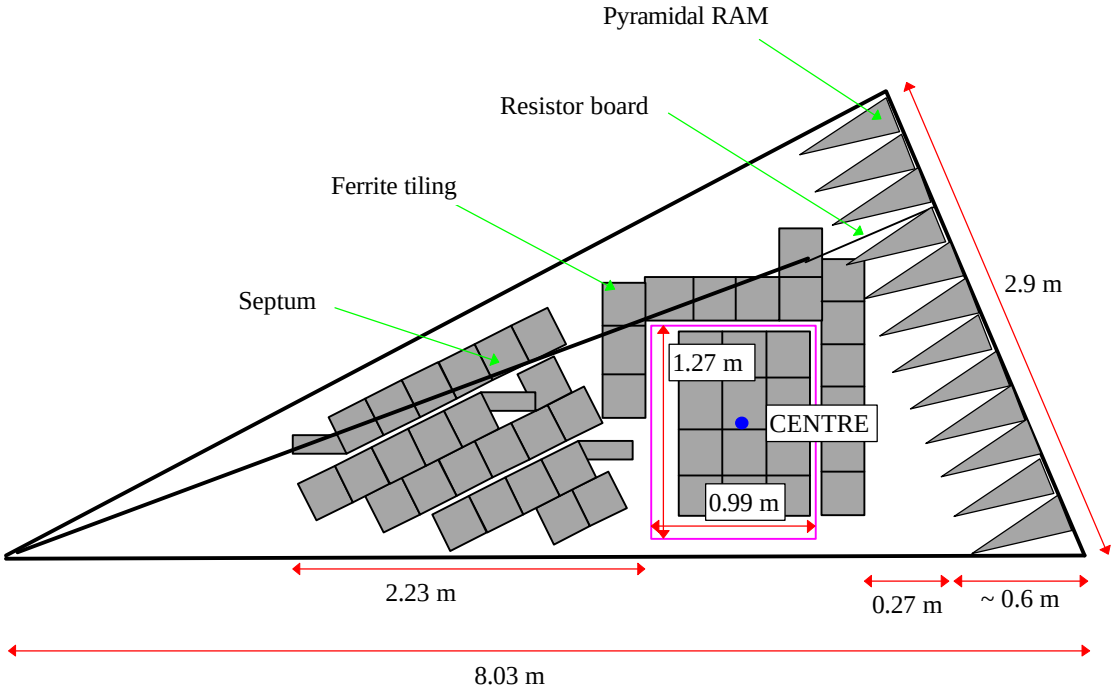

Figure 5 : Configuration of tiling on side wall with door.

This wall holds 53 blocks of 3×3 tiles placed so that they are parallel to the ceiling of the GTEM. A small panel was removed from the side of the door where the string was led out to the motor via the pulley system.

2.4 Analysis of data

The VB program "GTEM Scanner.vbp" produces an output file for each height, and these files contain the transverse positions, the frequency and the input power measured by the power sensor, as well as the orthogonal **E**-field components and the isotropic value. These are converted to Excel files and then a macro is used to convert the data to a more user-friendly format. For our purposes this meant creating a pivot table of transverse position against height for each component at each frequency. The isotropic field data was recorded but not processed. This was repeated for each set-up, i.e. when the GTEM was untiled, half tiled and fully tiled. This gave a total of 90 graphs, so not all of these are included in the results section for simplicity.

2.5 Measuring the longitudinal component at the cell centre

The process described above produces detailed field mapping of the cell and the effect of tiling over a large measurement plane surrounding the central point. This is useful to examine whether tiling the cell can extend the area in which the field is acceptably uniform. It is also a useful tool for visualising the **E**-field but cannot be used to examine the effect on the longitudinal cross-polar component with sufficient resolution as the frequency step of 100 MHz is too large. Previous measurements have been carried out using the FP-2000 in the untiled cell (See NPL Report CETM S22) using a

similar control program which measures at one position and uses a feedback loop from the power meter so that the power entering the cell produces the same **E**-field value at each frequency. This was repeated in the fully tiled cell.

Two measurement runs were carried out at the centre of the cell using finer frequency sweeps, from 30 MHz to 250 MHz in 1 MHz steps and also from 30 MHz to 1 GHz in 10 MHz steps. This allows closer examination of the longitudinal component at around 125 MHz. Comparisons of data produced in the tiled and untiled cell can be used directly to evaluate the effect of ferrite absorbers on the longitudinal cross-polar component of the **E**-field.

2.6 Further use of data

The scanner itself has other advantages as well as simply reducing measurement time. Foremost of these is that when the probe is half way between the septum and the floor one of its axes is at the angle at which the E-field is at its theoretical maximum rather than vertical, as it has been with previous measurements (e.g. CETM report S22). This should prove useful for measuring with single axis probes such as the Tokin sensor, a dipole sensor with fibre-optic cables that will not cause any field perturbation. The accuracy of the positioning of the scanner is $\pm$ 5 mm, so at the maximum frequency of 1 GHz this is equivalent to $\lambda/60$, which can be considered negligible. The extent of the field-mapping exercise should provide a good basis for later comparisons of different field probes used in the cell.

3. Results and Analysis

3.1 Field mapping results

This section contains the surface plots of each **E**-field component at the minimum and maximum frequencies, 100 MHz and 1 GHz respectively. Note that the plots of the vertical and transverse components have the same scale, from 0 to 18 Vm^{-1} , whereas the plots of the longitudinal component are from 0 to 4 Vm^{-1}.

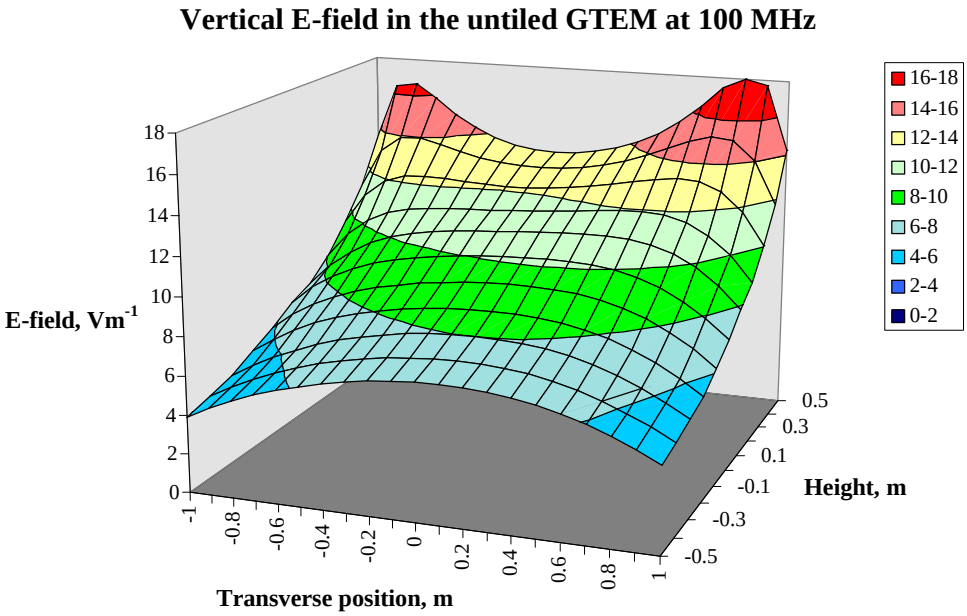

Figure 6.

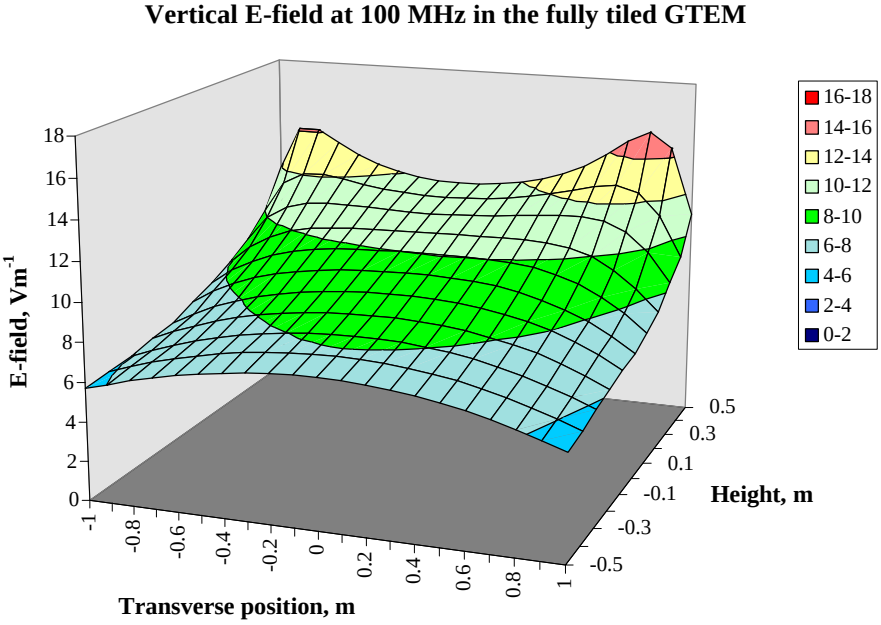

Figure 7.

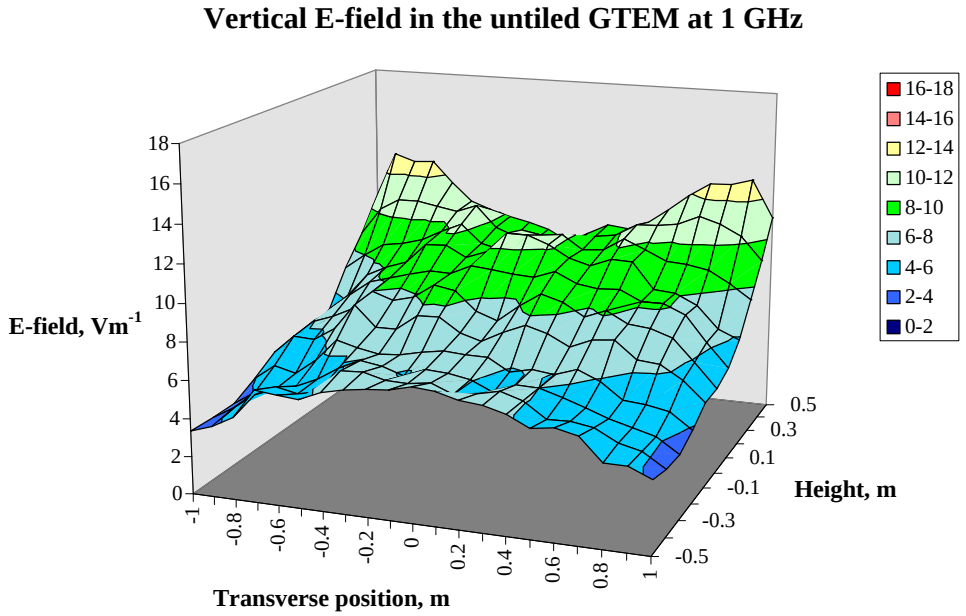

Figure 8.

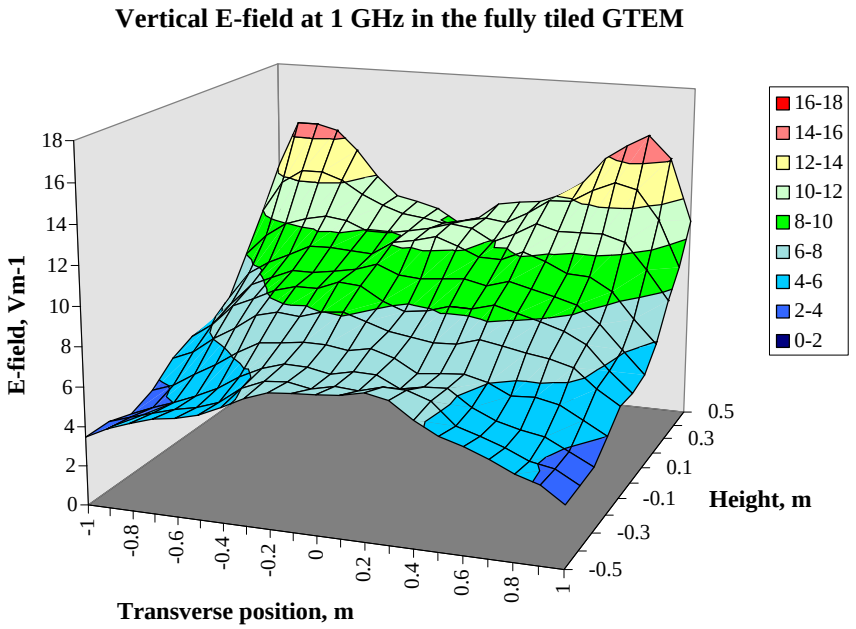

Figure 9.

Figures 6 to 9 show that the overall pattern for both the tiled and untiled cell are similar. The field increases slowly as height of the probe in the cell is increased and also shows peaks at the points closest to the edges of the septum. The plots at 100 MHz are noticeably smoother than those taken at 1 GHz, which is probably a result of higher order mode propagation. At 100 MHz the range of **E**-field values is greater in the untiled cell than the tiled (from 3.92 to 18.26 Vm^{-1} in the untiled GTEM compared to 5.36 to 15.28 Vm^{-1} in the tiled cell). At 1 GHz the reverse is true, the **E**-field

varying from 3.36 to 13.06 Vm^{-1} in the untiled cell, and from 3.12 to 15.3 Vm^{-1} in the fully tiled cell. There is no obvious trend.

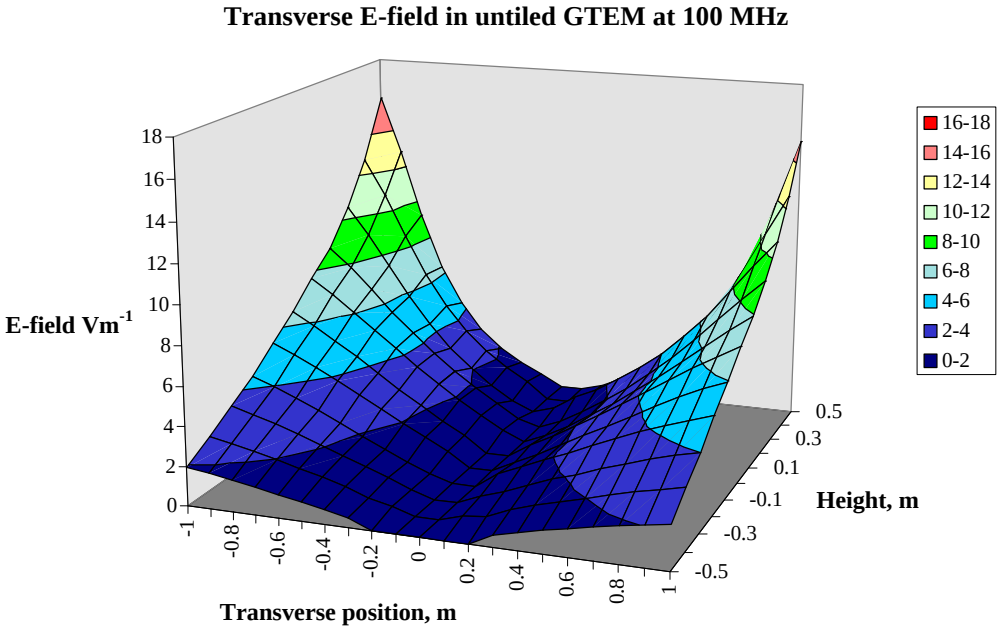

Figure 10.

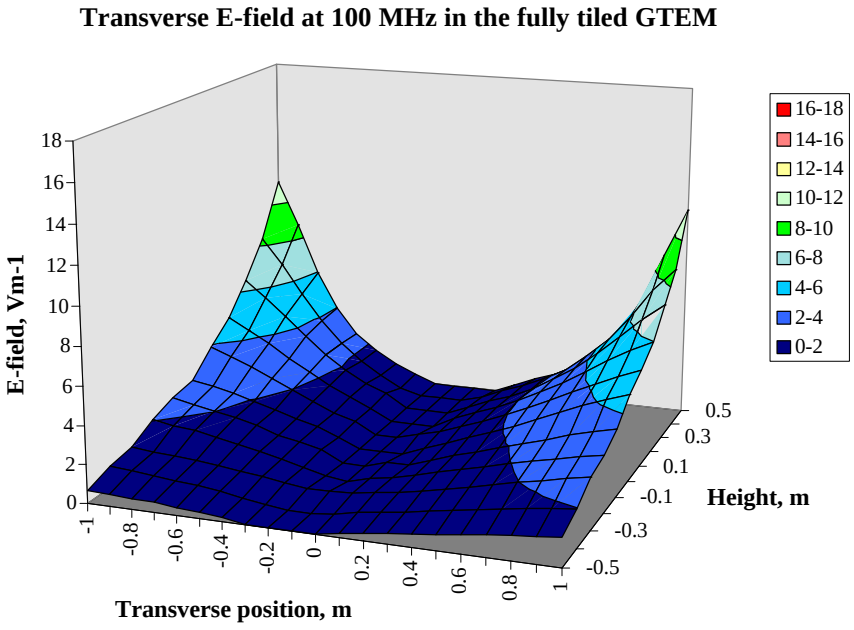

Figure 11.

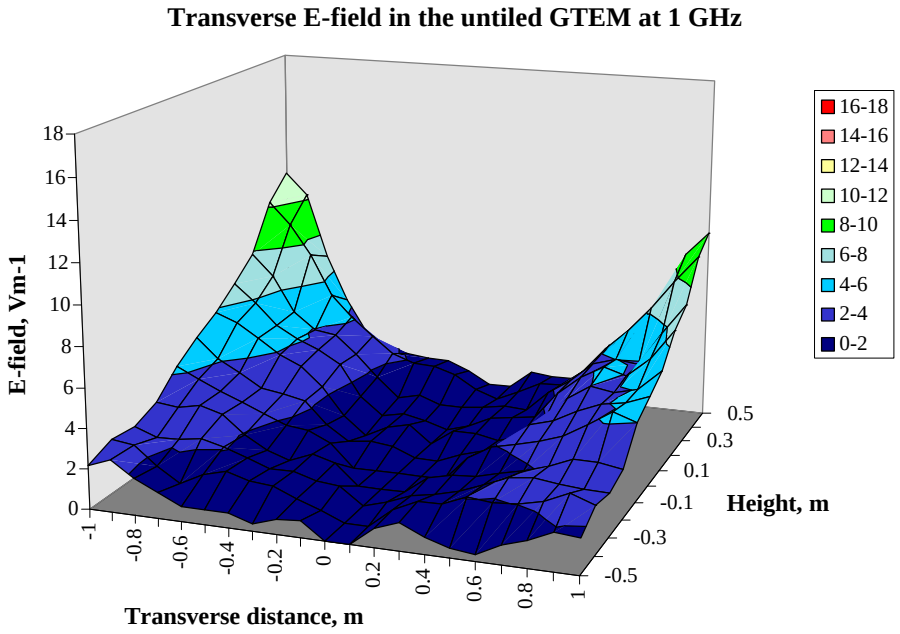

Figure 12.

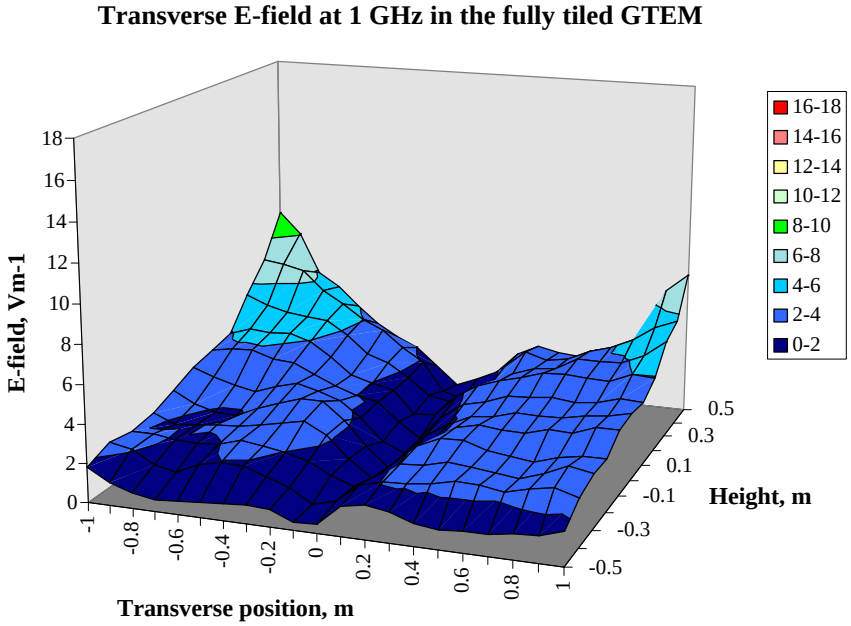

Figure 13.

Again the plots are both smoother at 100 MHz than 1 GHz. The general trend is a very small transverse component along the longitudinal axis, increasing slightly with height. Moving in the transverse direction, the transverse component increases approaching the edges of the septum. This is due to fringing effects, and is approximately symmetrical about the longitudinal axis. At 100 MHz the addition of the ferrite tiles does appear to reduce the maximum **E**-field and extend the area in which the field is under 2 Vm^{-1}. However, this effect can only be considered significant if the longitudinal component is also substantially reduced over this area. The longitudinal component is shown in Figures 14 and 15 below.

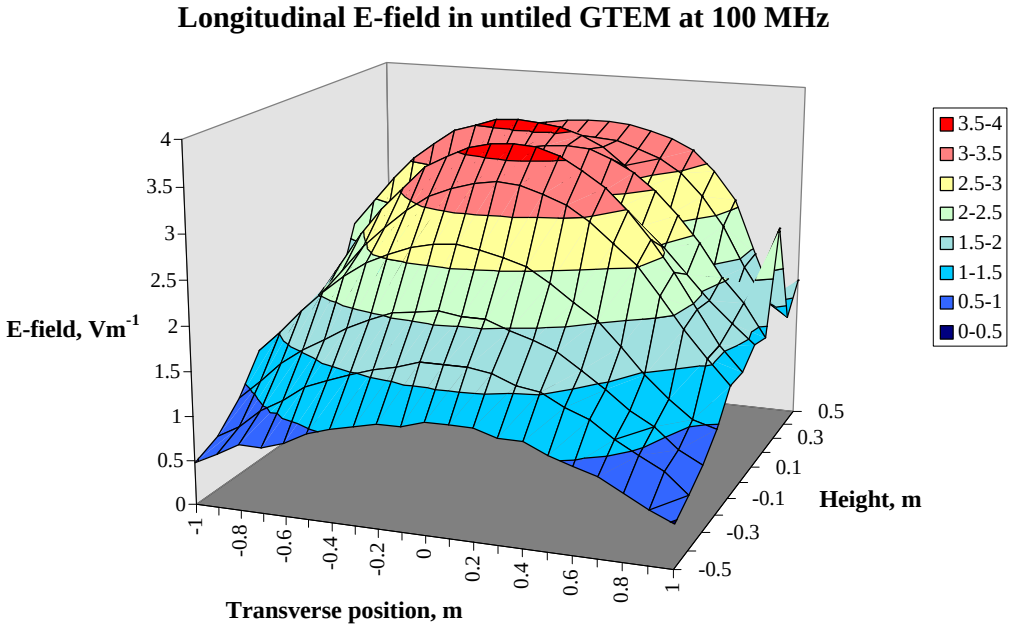

Figure 14.

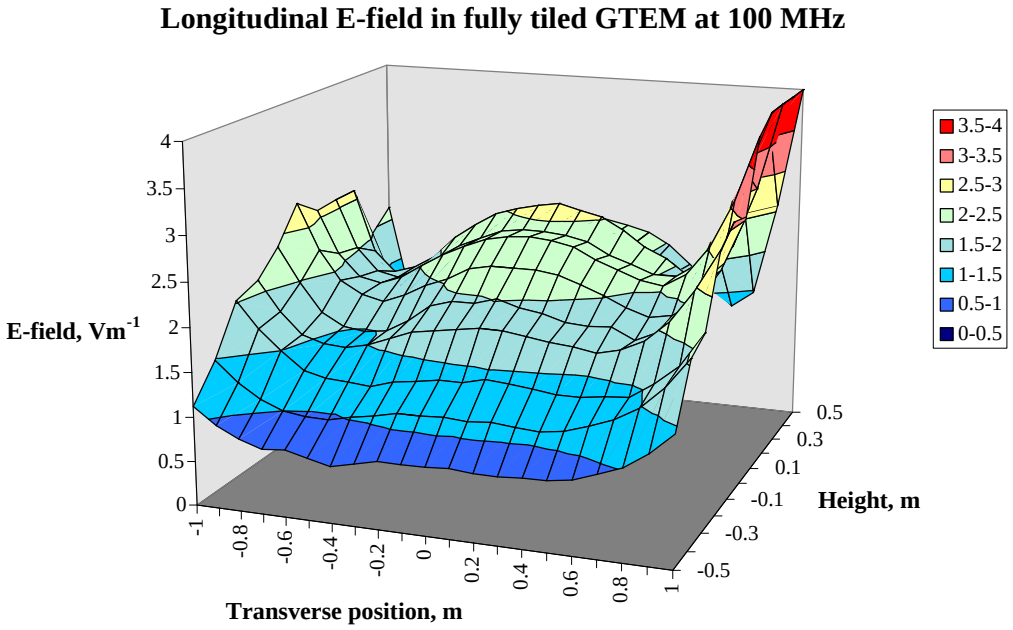

Figure 15.

The longitudinal component detected in the untiled GTEM 1750 appears at 125 MHz. The graphs above show what appears to be a standing wave. Addition of the ferrite tiles shows the peak values decrease by about 1 Vm^{-1} at 100 MHz. The effect of the longitudinal component at the central position is examined in more detail later. Clearly, the component is not eliminated entirely, and above 300 MHz, there seems to be no reduction in the longitudinal component as a result of the ferrite tiles. The scans carried out at 1 GHz in both the tiled and untiled cells are included in Figures 16 and 17 below. From this data it is hard to argue that tiling the cell suppresses the cross-polar components enough to extend the measurement area of the cell. Having said that,

at the higher frequencies, the longitudinal component is less that 2 Vm^{-1} across the entire scan area and shows no clear trend in any direction.

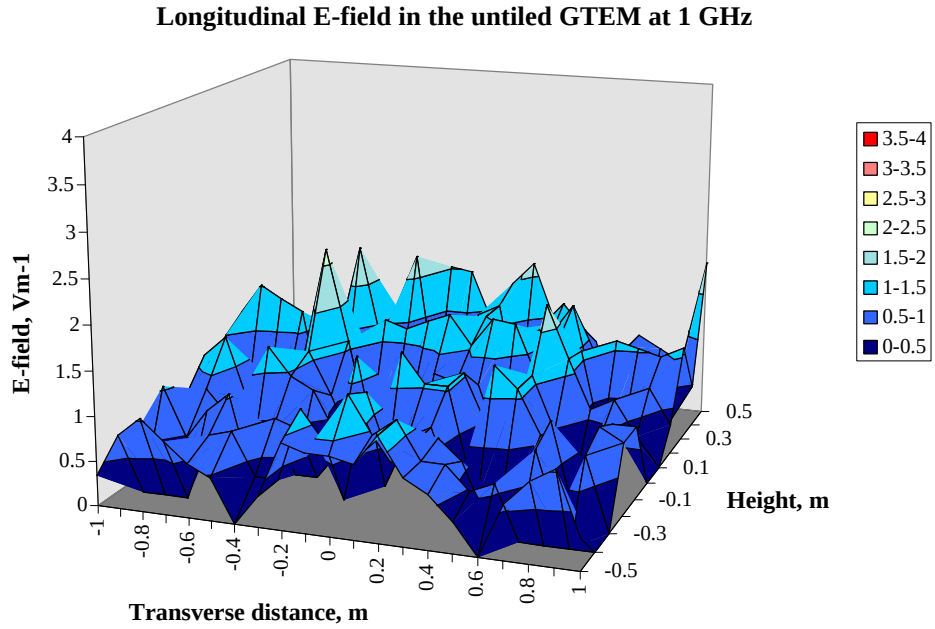

Figure 16.

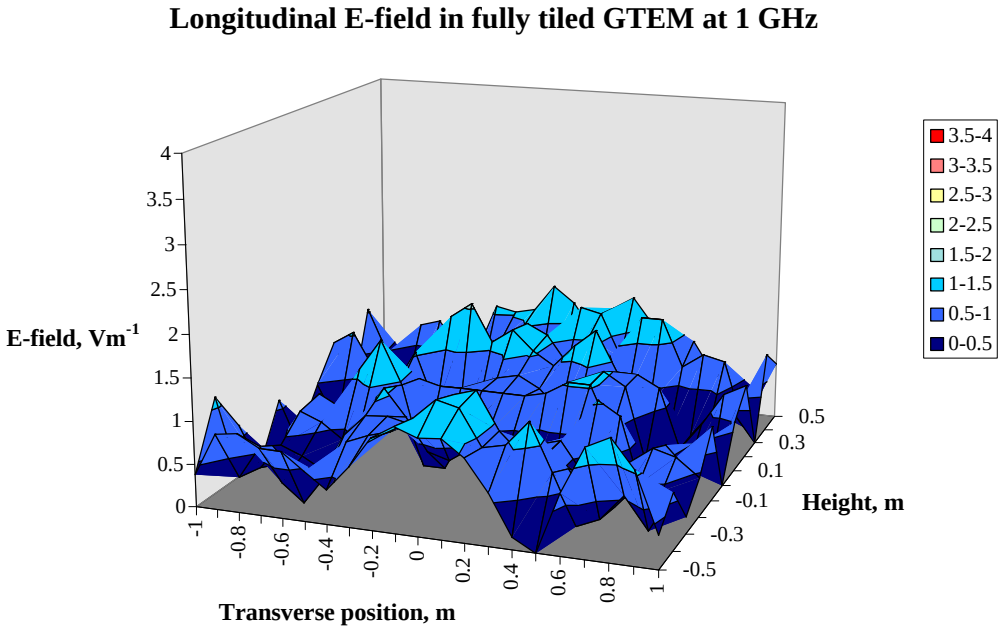

Figure 17.

3.2 Result of tiling on the longitudinal component

As discussed in the measurement section, to test the effect of the tiling on the longitudinal component, a measurement set was carried out at the centre of the cell using a finer frequency sweep of 1 MHz. This was done using a slightly different VB program, control.vbp, developed for an earlier project, to duplicate measurements already carried out in the empty cell. The frequency range was from 30 MHz to 250 MHz. Similarly, a measurement was carried out from 30 MHz to 1 GHz in 10 MHz steps. This program involves an initial calibration so that the output power from the signal generator maintains a constant vertical **E**-field value in the cell, which is user-defined, over the entire frequency range. For this report the **E**-field was set to 8 ± 0.2 Vm^{-1}. The values recorded for each orthogonal **E**-field component are shown in Figure 18 and 19.

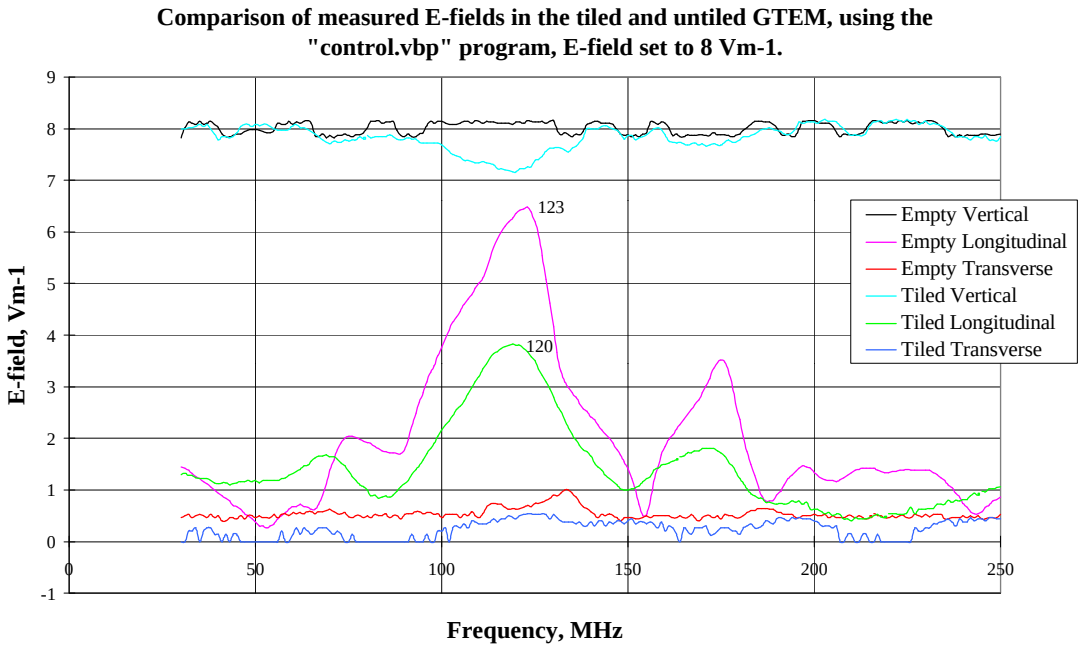

Figure 18 : Orthogonal components of E-field at the centre position in the tiled and untiled GTEM cell in 1 MHz steps.

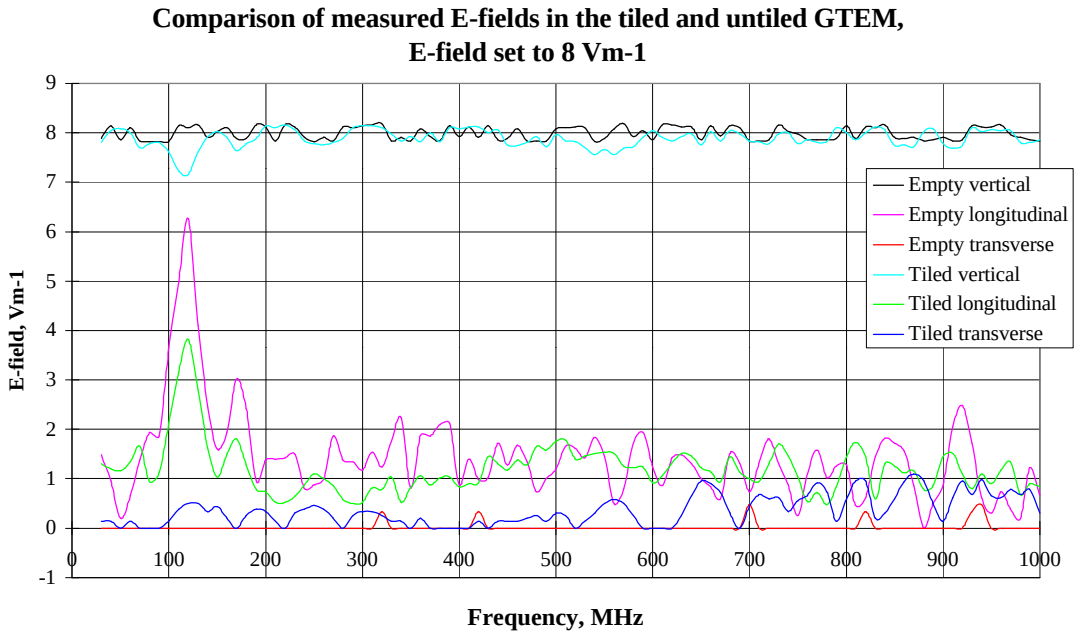

Figure 19 : Orthogonal components of E-field in the tiled and untiled GTEM cell in 10 MHz steps.

Figures 18 and 19 show that there is a reduction in the longitudinal peak, and also that it appears to have shifted down slightly in frequency. There is a slight discrepancy at between about 100 and 140 MHz where the vertical field in the tiled cell falls below the requisite 8 Vm^{-1}, which could be due to the amplifier not being able to provide enough power to produce this field value. By taking the ratio of the longitudinal component to the vertical component and converting to dB, this discrepancy is taken out, so the reduction in the longitudinal component can only be as a result of the ferrite tiling.

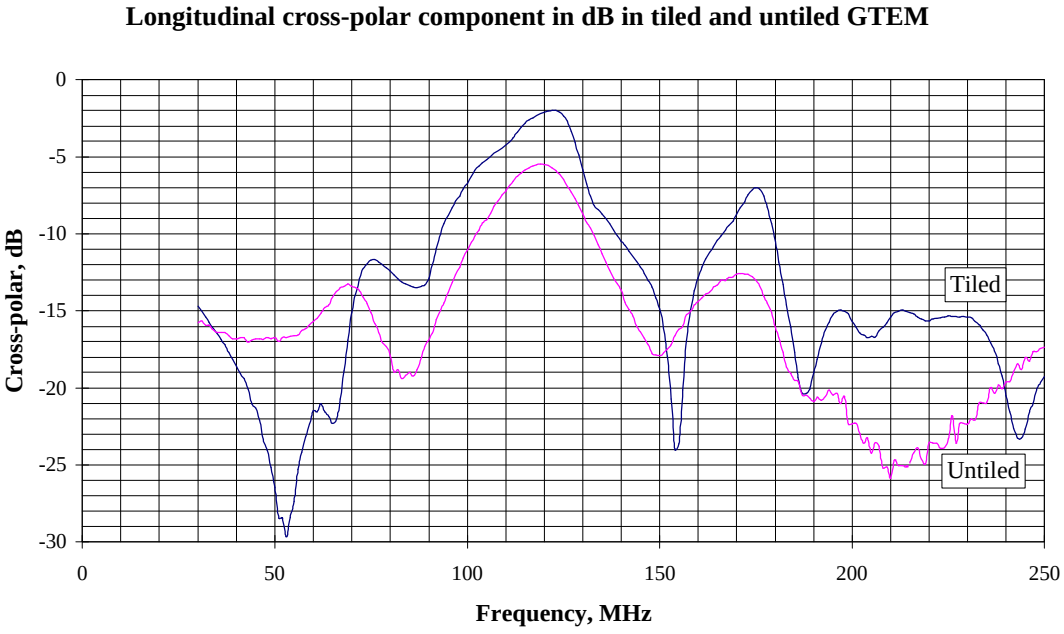

Figure 20.

The graph above shows that while the cross-polar peak it is reduced by 3.5 dB by the addition of ferrite tiles. The peak now appears at 119 MHz, and, at it's maximum, the longitudinal component is now 5.5 dB down on the vertical, compared to -2.0 dB in the untiled cell. This reduction can be considered significant. Figure 20 also shows that either side of the peak the longitudinal component is reduced and while the smaller peaks still appear, their magnitude is reduced.

3.3 Calculability of tiled GTEM

The addition of the ferrite tiles has an effect on the impedance of the cell. This was quantified by TDR measurement carried out in the cell before and after it was tiled. Prior to tiling the GTEM, the impedance at the centre of the cell was measured as 49.7 Ω, and after tiling 52.0 Ω. It is necessary to test whether the cell remains calculable with the additional absorber in place. For the measurements taken as described above, the **E**-field in the centre of the cell remains constant across the frequency range, at 8 Vm^{-1}. The **E**-field can also be calculated from the input power measurement using the equation

$$E = \frac{\sqrt{P_{in} Z_0}}{d} \qquad [1]$$

where P_{In} is the input power, Z_0 is the real part of the complex impedance with the values quoted above, and d is the floor to septum separation. This equation is a quasi-static approximation and only applies at the midway position between the septum and the floor of the cell. It also assumes a perfect input match to the cell. This was carried out for both untiled and tiled cell configurations. This value was then subtracted for the measured field at each frequency, and this is shown in Figure 21.

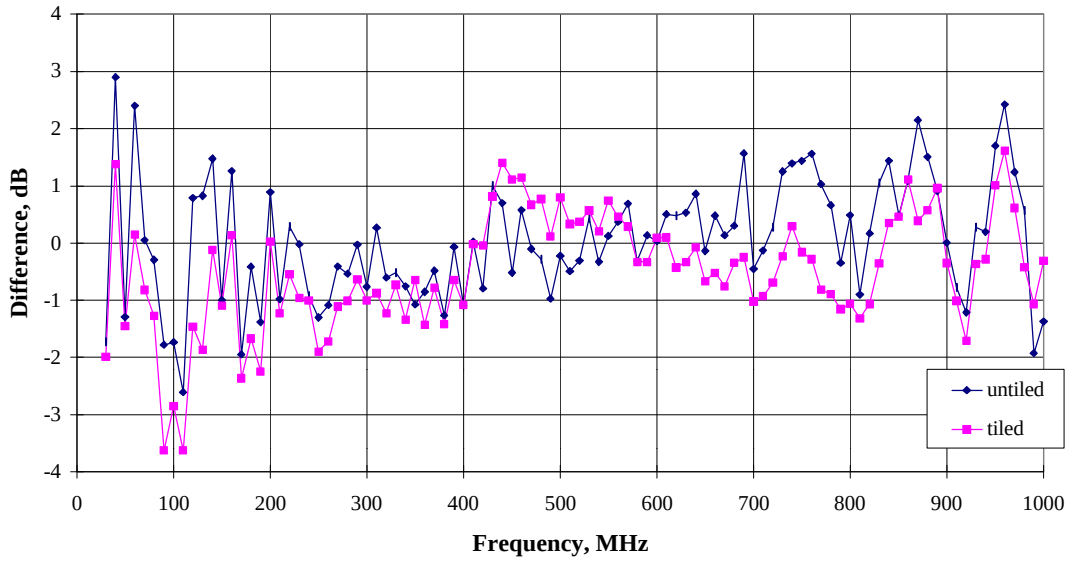

Figure 21 : Measured vertical E-field minus E-field calculated from the input power using Equation [1] up to 1 GHz.

It can be seen from Figure 21 that tiling the GTEM does not make it less calculable than it was before tiling. Unfortunately it does not appear to significantly improve the calculability either. The result obtained using the finer frequency sweep with 1 MHz steps is shown in Figure 22.

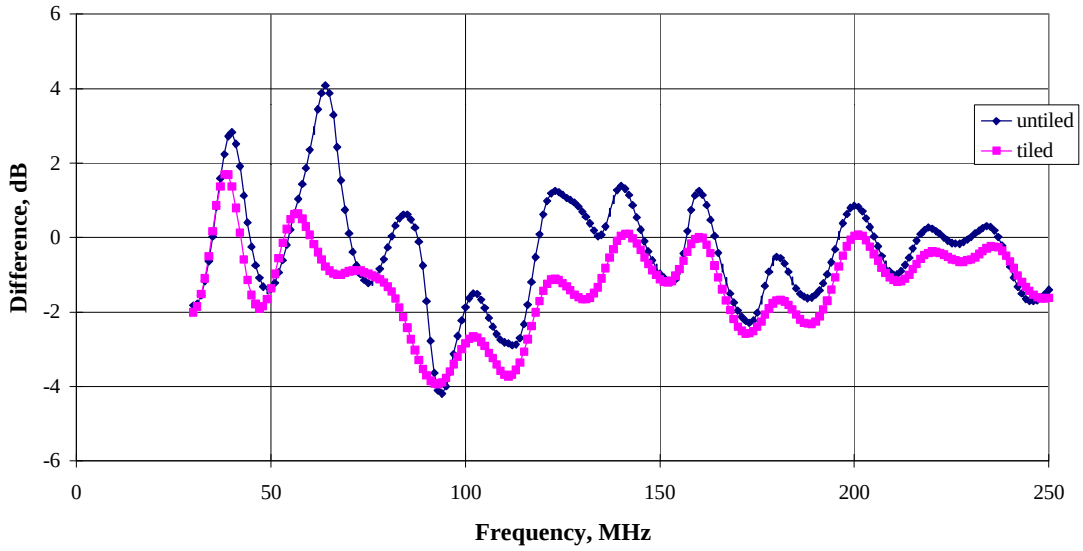

Figure 22 : Measured E-field minus E-field calculated from the input power using Equation [1] in 1 MHz steps.

This graph appears to show a slight improvement to the calculability of the GTEM at the lower end of the frequency range. The tiled plot is lower, which shows that some

power absorption is taking place. The untiled plot is more centred about 0 dB and therefore is more calculable in this frequency range, though a systematic correction could be applied. Figure 21 shows this is true up to about 400 MHz. Both tiled and untiled results show agreement between measured and calculated values to within ± 2 dB over most of the frequency range. However the presence of the tiles cannot be said to produce a consistent improvement in the calculability of the GTEM cell over the entire frequency range.

4. Conclusions

It is clear from the data above that tiling the cell does have benefits. The longitudinal component of the electric field has been significantly reduced by placing absorber tiles in the cell. The positioning of the ferrites on the cell walls was arbitrary and it is possible that optimising the positions of the tiles may improve this aspect of the performance. However, this would involve a certain amount of trial and error as we do not yet have a working mathematical model of a tiled GTEM. NPL are currently working towards developing such a model.

It does not appear from this investigation that tiling will reduce sufficiently the cross-polar components at positions other than the centre of the cell to justify extending the measurement area. Measuring the change in impedance in the cell and using this to test the calculability of the GTEM before and after tiling does show an improvement up to about 400 MHz. Above this frequency there is no consistent improvement or deterioration resulting from the tiling.

The field-mapping exercise increased our knowledge of the field in the empty GTEM and demonstrates that the scanner works. This is useful should we make any more changes to the GTEM. If the scanner is used in future it would be worth creating a data-processing program to make the large amount of data more manageable.

Finally the FP-2000 probe is a small instrument with fibre optic cables which causes minimal perturbation to the **E**-field. Real EUTs are likely to be larger and therefore cause more field scattering. With the ferrite grid tiles lining the GTEM walls, any scattering produced by a large EUT may be reduced as well, and it is possible that the tiles may be more effective for a large EUT than for a small sensor. By placing such an object into the GTEM in front of the FP-2000 and repeating the scan measurements, then removing the tiles and carrying the scan out again it should be possible to quantify the effect of the absorber tiles on the field scattered by the EUT. These can in turn can be compared with FAR measurements. This is an area that NPL intends to investigate in the future.